IIIIII Microgravity Experiments by Aircraft Parabolic Flights IIIIII
(Review)

Study of Cylindrical Dusty Plasmas in PK-4J; Theory and Simulations

Hiroo TOTSUJI [1], Chieko TOTSUJI [2], Kazuo TAKAHASHI [3] and Satoshi ADACHI [1]

Abstract

An overview on theoretical works and numerical simulations on dusty plasmas with cylindrical symmetry is presented. The main purpose of these works has been to investigate strongly coupled dusty plasmas which are expected to be realized in the planned experiments by PK-4 on the International Space Station and experiments by PK-4J, a similar apparatus constructed here. The distribution of dust particles is analyzed, both analytically and numerically, first on the basis of the drift-diffusion equations as continuum and then numerical simulations have been performed, taking the effect of discreteness into account.

Keyword(s): cylindrical dusty plasma, PK-4J, drift-diffusion equation, numerical simulation

1. Introduction

In the investigations of fundamental properties of strongly coupled Coulomb and Coulomb-like systems, dust (fine) particles of micron size in plasmas have been very useful [1,2]. They are easily traced by scattering of laser light and strong coupling is realized due to negative charges of large magnitude on a particle. In experiments, it is necessary to have a three-dimensional homogeneous system with simple geometry. These particles, however, are still macroscopic and, in order to avoid the effect of gravity, experiments on the International Space Station (ISS) have been performed by the apparatus PK-3 Plus [3].

After PK-3 Plus, the project PK-4 on the ISS is now in progress [4]. In PK-4, the plasma is generated by a discharge in a long cylindrical tube. This kind of plasma where the cylindrical symmetry and the uniformity along the axis are expected is one of strong candidates for three-dimensional homogeneous system with simple geometry. Structures of these apparatus are shown in **Fig. 1**.

As one of JAXA Working Groups, we have been working on such cylindrical dusty plasmas in order to make proposals of possible interesting themes for PK-4 experiments. We here summarize results of our theoretical and simulation works. An overview of our experimental works based on the similar apparatus PK-4J is also given in the same issue.

We consider the system of dust particles in a plasma with the cylindrical symmetry. We assume that the discharge is maintained by the dc electric field along the axis and also that the polarity of field is alternating with the frequency around 1 kHz to prevent the flow of dust particles along the axis. The frequency of polarity
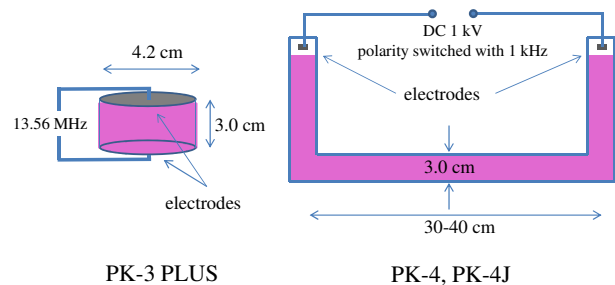
Fig. 1   In PK-3 PLUS (left), plasma is generated by rf discharge. In PK-4 and PK-4J (right), dc discharge with polarity switching generates plasma and behavior of dust particles is observed in the central straight part which is a long cylinder.

change is much larger than characteristic frequencies of dust particles and much smaller that those of ions or electrons: Electrons and ions follow alternating electric field but the field is averaged to zero for dust particles.

We analyze the behavior of dust particles on the basis of the drift-diffusion equations assuming electrons, ions, and dust particles have different temperatures. We then analyze the effect of discreteness of dust particles, correlation and structure formations, by numerical simulations.

2. Basic Equations and General Properties of Solutions with Cylindrical Symmetry

2.1 Drift-Diffusion Equations

1   Institute of Space and Astronautical Science, Japan Aerospace Exploration Agency, 2-1-1 Sengen, Tsukuba, Ibaraki 305-8505, Japan

2   Kogakuin University, Nishishinjuku, Shinjuku-ku, Tokyo 163-8677, Japan.

3   Kyoto Institute of Technology, Matsugasaki, Sakyo-ku, Kyoto 606-8585, Japan

(E-mail: totsuji-09@t.okadai.jp)

Our system is composed of plasma (electrons and ions) and dust particles. We denote physical quantities of these components by suffixes e, i, or α, α being the species of dust particles. For densities $n_{e,i,\alpha}$ and flux densities $\boldsymbol{\Gamma}_{e,i,\alpha}$, we have equations of continuity,

$$\frac{\partial n_e}{\partial t} + \nabla \cdot \boldsymbol{\Gamma}_e = \frac{\delta n_e}{\delta t}, \tag{1}$$

$$\frac{\partial n_i}{\partial t} + \nabla \cdot \boldsymbol{\Gamma}_i = \frac{\delta n_i}{\delta t}, \tag{2}$$

and

$$\frac{\partial n_\alpha}{\partial t} + \nabla \cdot \boldsymbol{\Gamma}_\alpha = 0. \tag{3}$$

Right-hand sides express the generation and the loss of plasma. In the drift-diffusion approximation, flux densities are expressed by diffusion coefficients $D_{e,i,\alpha}$ and mobilities $\mu_{e,i,\alpha}$. We assume that these are related via the Einstein relations with the temperature of corresponding component, $T_{e,i,\alpha}$.

The force acting on a dust particle of species α with the charge $-Q_\alpha e$ is given by

$$\boldsymbol{F}_\alpha = (-Q_\alpha e)\boldsymbol{E} + \boldsymbol{F}_\alpha^{id}, \tag{4}$$

where the first term is due to the electric field $\boldsymbol{E}$ and the second term is the ion drag force. The ion drag force has been investigated extensively [1] and it has been shown that the magnitude is approximately proportional or inversely proportional to the ratio of the average ion drift velocity u_i and the ion thermal velocity $v_i = (k_B T_i/m_i)^{1/2}$:

$$F_\alpha^{id} \propto \frac{u_i}{v_i} \left(\frac{u_i}{v_i} < 1 \right), \quad F_\alpha^{id} \propto \frac{v_i}{u_i} \left(\frac{u_i}{v_i} > 1 \right). \tag{5}$$

We express this force by appropriately choosing proportionality constants.

2.2 Generation and Loss of Plasma and Charging of Dust Particles

In our system, the axial electric field with alternating polarity is applied. The electron motion along the axis generates the plasma by the impact ionization. We express the generation rate per volume in the form $c_g n_e$ with the coefficient c_g which is assumed to be constant in the system.

The plasma is lost by recombination at the boundary of the system (wall) or the surface of dust particles (we neglect the recombination in the plasma bulk). The charge of the particle α is determined by the balance between the electron current $I_{e\alpha}$ and the ion current $I_{i\alpha}$, $I_{i\alpha} = I_{e\alpha}$. The typical value of Q_α amounts to 10^3 or even 10^4. Denoting $I_{i\alpha} = I_{e\alpha}$ by c_α, we have the generation and loss of the plasma in the form

$$\frac{\delta n_i}{\delta t} = \frac{\delta n_e}{\delta t} = c_g n_e - \sum_\alpha c_\alpha n_\alpha. \tag{6}$$

The charge of a particle is approximately proportional to the radius and the electron temperature and is also influenced by the ion mean free path [1]. We take these known effects into account.

2.3 Stationary State with Cylindrical Symmetry

We assume that our system is stationary and cylindrically symmetric. In this case, $\boldsymbol{E}$, $\boldsymbol{F}_\alpha^{id}$, and $\boldsymbol{u}_i$ have only the radial component E, F_α^{id}, and u_i, respectively, and we introduce the factors f_α and f_i related to the ratio of the magnitudes of the ion drag force to the electric field force by

$$f_\alpha = \frac{F_\alpha^{id}}{Q_\alpha e E}, \qquad f_i = \sum_\alpha f_\alpha \frac{Q_\alpha n_\alpha}{n_i}. \tag{7}$$

In terms of $s = R^2$ where R is the radius, we have

$$2D_e \frac{d}{ds} s \left[-2\frac{d}{ds} n_e - \frac{eE}{s^{1/2} k_B T_e} n_e \right] = \frac{\delta n_e}{\delta t}, \tag{8}$$

$$2D_i \frac{d}{ds} s \left[-2\frac{d}{ds} n_i + (1-f_i)\frac{eE}{s^{1/2} k_B T_i} n_i \right] = \frac{\delta n_i}{\delta t}, \tag{9}$$

and

$$2D_p \frac{d}{ds} s \left[-2\frac{d}{ds} n_\alpha - (1-f_\alpha)\frac{Q_\alpha e E}{s^{1/2} k_B T_\alpha} n_\alpha \right] = 0. \tag{10}$$

When the neutral gas density (which determines the generation rate) is given, these equations, the equation for particle charging, and the Poisson's equation determine n_e, n_i, n_α, Q_α, and E.

3. Behavior of Solutions

We here analytically discuss behavior of solutions.

3.1 Without Dust Particles

In this case, the above equations give the ambipolar diffusion equation for $n \sim n_e \sim n_i$,

$$\frac{d}{ds} s \frac{d}{ds} n + \frac{1}{4R_a^2} n = 0, \tag{11}$$

with the solution expressed by the Bessel function

$$n = n(R=0) J_0(R/R_a). \tag{12}$$

Here R_a is related to the ambipolar diffusion coefficient D_a

$$D_a = \frac{\mu_e D_i + \mu_i D_e}{\mu_e + \mu_i} \tag{13}$$

via $R_a^2 = D_a/c_g$. We assume that the boundary of the system (the discharge tube radius) R_w corresponds to the first zero of $n(R)$ as $R_w = 2.41 R_a$.

The electrostatic potential Ψ is given by

$$\Psi(R) - \Psi(0) \approx \frac{k_B T_e}{e} \ln J_0(R/R_a) \tag{14}$$

and the charge density around the center is

$$-\varepsilon_0 \Delta \Psi = \frac{1}{A} \left[1 + \frac{1}{4} \frac{R^2}{R_a^2} + \dots \right] en(0). \tag{15}$$

Here the parameter A is defined by

$$A = k_e^2 R_a^2, \tag{16}$$

k_e being the electron Debye wave number

$$k_e^2 = \frac{e^2 n(0)}{\varepsilon_0 k_B T_e}. \tag{17}$$

Usually both the electron and the ion Debye lengths are much smaller than the system size represented by R_a and $A \gg 1$. The space charge is thus controlled by the electron Debye length and the quasi-charge-neutrality is satisfied to the order of $1/A$ relative to $en(0)$.

3.2 General Behavior near Axis

We here consider the case of dust particles of one species α. Assuming the normalized charge density at $s = 0$

$$\Delta = \frac{n_i(0) - n_e(0) - Q_\alpha(0)n_\alpha(0)}{n_e(0)}, \tag{18}$$

we obtain the solutions in the form of expansions with respect to $s = R^2$. Since $A \gg 1$, we expand Δ in the form

$$\Delta = \frac{a_1}{A} + \frac{a_2}{A^2} + \dots. \tag{19}$$

In order for the solution to behave properly, a_1 is shown to be inversely proportional to a factor including $Q_\alpha^2 T_e n_\alpha / T_\alpha n_e$. When $n_\alpha(0) = 0$, a_1 reduces to the case of no particles $a_1 \approx 1$. We implicitly assume that the charge density of dust particles, $Q_\alpha n_\alpha$, is small but not much smaller than electrons or ions. Since Q_α is of the order of 10^3 or more, the above factor becomes much larger than unity and we have $a_1 \ll 1$. The electron density around the axis is then given by

$$\frac{n_e(s)}{n_e(0)} = 1 - \frac{a_1}{4} \frac{s}{R_a^2} + \dots. \tag{20}$$

The coefficient of the second term, $a_1/4$, is much smaller than unity and also much smaller than those appearing in similar expansions for $n_i(s)/n_e(0)$ and $Q_\alpha n_\alpha(s)/n_e(0)$, the latter two being the same. The charge density around the axis is thus given by

$$\frac{n_i(s) - n_e(s) - Q_\alpha(s)n_\alpha(s)}{n_e(0)} = a_1 \left(\frac{1}{A} + \frac{1}{4} \frac{s}{R_a^2} \right) + \dots. \tag{21}$$

Since $a_1 \ll 1$, the charge neutrality near the axis is satisfied to a much better accuracy than the case without particles, (15). We may intuitively understand this effect as the increased Debye wavenumber which is generally given as the sum of *charge squared* times density (divided by the temperature).

We thus expect that the almost flat electron density, the enhanced charge neutrality near the axis, and the compensation of increased negative charges of dust particles by ions. These are also confirmed by numerical solutions shown below. Though the above analysis is for the case of cylindrical symmetry, we expect these features generally hold in the general case where we have appreciable amount of dust particles.

3.3 Void Formation Condition

In experiments under microgravity by PK-3 Plus, they often observed the existence of central space called 'void' where we have no dust particles[5]. Since, in experiments by PK-4J, we would like to have systems of dust particles which is as large as possible without void, the condition for the formation of voids is an important issue.

Two kind of forces act on dust particles; inward force by the electric field and outward force by the ion drag. When the latter exceeds the former, dust particles cannot stay around the axis and the void appears. The condition for the appearance of void is then given by

$$f_\alpha(0) = \left[\frac{F_\alpha^{id}}{Q_\alpha eE} \right]_{s \to 0} > 1 \quad \text{when} \quad n_\alpha(0) = 0. \tag{22}$$

This is rewritten in terms of basic parameters into a condition for the product

$$Q_\alpha(0)n_e(0) > [Q_\alpha(0)n_e(0)]^c, \tag{23}$$

where $[Q_\alpha(0)n_e(0)]^c$ is expressed by T_e/T_i and ℓ_i, the latter being the ion mean free path determined by the the neutral gas density n_n (or the pressure p_n and the temperature T_n).

Since the charge Q_α is approximately proportional to the radius of dust particles r_α and the electron temperature T_e, the critical electron density $n_e^c(0)$ for void formation is given by

$$n_e^c(0) \propto \frac{T_i^2}{T_e} \frac{p_n}{T_n} \frac{1}{r_\alpha}. \tag{24}$$

Actually, the charge Q_α also depends on the electron density and the neutral gas pressure and (23) gives a nonlinear equation. The result of numerical analysis of this condition has been compared with numerical analysis of drift-diffusion equations.

3.4 Dust Particles of Two Species and Void-Like Structure

Let us consider the case where there exist dust particles of two species α and β with radii r_α and r_β, $r_\alpha > r_\beta$, both satisfying the no-void condition. Since the charge of a dust particle is proportional to its radius, we have $1 > f^\alpha > f^\beta$ and the effect of ion drag on the species α is stronger than the one on the species β. The species α is then located in the outer domain and the species β is distributed in the inner domain. As a distribution of α, there is a void at the center filled with smaller dust particles of β.

Table 1   Parameters

$k_B T_e/e$	$(1 \sim 3)$ eV
T_i	300 K
T_α	300 K
$n_e(0)$	$(1 \sim 3) \cdot 10^8 \mathrm{cm}^{-3}$
r_p	$(1 \sim 3)\ \mu$m
R_w	1.5 cm
$R_a = R_w/2.4$	0.63 cm

Table 2   Derived parameters

$\lambda_e(0) = (\varepsilon_0 k_B T_e/n_e(0)e^2)^{1/2}$	$7.43 \cdot 10^{-2}$cm
$(\varepsilon_0 k_B T_i/n_e(0)e^2)^{1/2}$	$7.44 \cdot 10^{-3}$cm
$A = (R_a/\lambda_e(0))^2$	$8 \sim 72$

4. Numerical Analyses of Drift-Diffusion Equations

Before the numerical treatment, we integrate both sides of equations with respect to s, noting the behavior of solutions $s = 0$. Starting from $s = R^2 = 0$ with some assumed value of Δ, we numerically integrate resultant equations and adjust Δ so as to have asymptotically vanishing distributions near the wall: Inappropriate values of Δ lead to divergence before reaching the wall. Solutions are quite sensitive to the value of Δ and numerical computations with very high accuracy are needed.

Values of basic parameters adopted in numerical analyses and corresponding characteristic parameters are listed in Table I and II, respectively. The typical radius of the discharge tube R_w is assumed to be around 1.5 cm and R_a is estimated by $R_a = R_w/2.41$.

4.1 Solutions Without Dust Particles

The solutions without dust particles are shown in **Fig. 2**. We observe that the known solutions are reproduced. The positive space charge increases with the radius, connecting to the domain of sheath near the outer boundary at $R = R_w$. The distribution functions near the wall, however, are not intended to be accurate, similarly to the description by the ambiploar diffusion equation: Since our interest is mainly in the behavior of dust particles around the axis, this gives no difficulty to our analyses.

Based on the equations for the moments of the distribution functions, we can describe the average ion and electron velocities as functions of radius including the sheath domain near the wall. It is shown that the ion drift velocity is sufficiently smaller than the ion thermal velocity at least in the domain $R < 0.5R_a$ and the description of flux densities by diffusion coefficients and mobilities is justified.

4.2 Dust Particles of One Species

Some examples of distribution functions, the charge density,
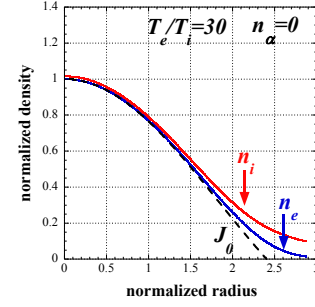
Fig. 2   Distribution of electrons and ions without dust particles
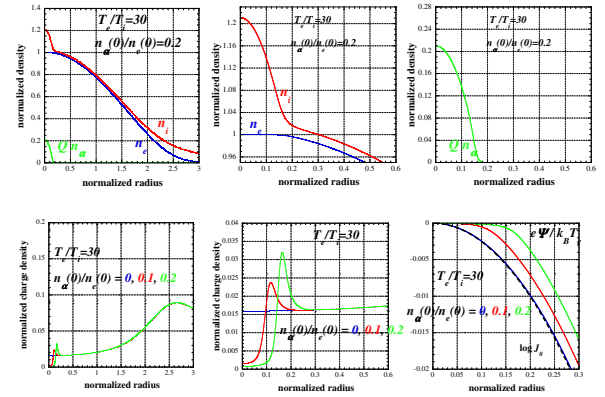
Fig. 3   Distribution of electrons, ions, and dust particles (top), charge density (bottom left and center), and electrostatic potential (bottom right)

and the potential are shown in **Fig. 3**. The radius of particle distribution increases with the density at the center. We observe the characteristic features described in Section 3 are confirmed in these results. At the radius where the density of dust particles vanishes and the electron distribution begins to decrease, we have the overshooting of the net positive charge density. When dust particles exist, the negative charge of dust particles is compensated by the increase of the ion density. Since the ion diffusion coefficient is larger than that of dust particles, the decay of dust particle density cannot be completely followed by the ions. This overshooting of ion distribution gives the overshooting of net charge density.

4.3 Formation of Void

With the increase of the electron density (at the center) $n_e(0)$, the increase of the dust particle radius r_p, or the decrease of the neutral atom density (the gas pressure) p_n, there appears the void at the center. When the void is formed at the center, the density of dust particles increases with the radius starting from very small values at the center. The critical values of the parameters are in good agreement with the numerical analysis of the condition discussed in Section 3. The condition of the void formation has
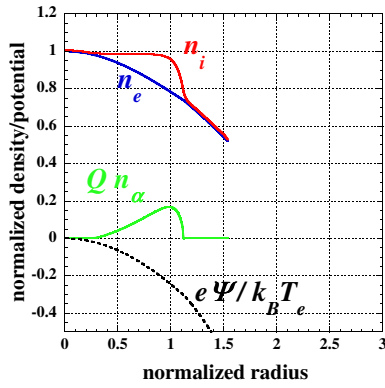
Fig. 4   Distribution with void

somewhat weaker dependence on T_e than rough estimation and is approximately expressed by

$$n_e^c(0)[\text{cm}^{-3}] \sim 10^7 \frac{p_n[\text{Pa}]}{T_e^{1/2}[\text{eV}]r_p[\mu\text{m}]}. \tag{25}$$

An example of the distribution near the critical condition is shown in **Fig.4**.

4.4   Dust Particles of Two Species

We have also analyzed some cases where there exist two species of dust particles. As is discussed in Section 3, we observe that smaller particles are distributed inside of larger particles.

5.   Simulation

In the previous sections, the behavior of dust particles in cylindrical discharge like PK-4 and PK-4J is analyzed on the basis of the drift-diffusion equations which give average distributions. In order to obtain their structure formations, it is necessary to take the effect of discreteness into account. The interaction between dust particles and its screening appear in this level of description for particles and the ambient plasma. We here show the results of structure formation obtained by numerical simulations of dust particles.

5.1   Potential

In the case of uniform system where average densities of electrons, ions, and dust particles satisfy the charge neutrality condition, dust particles are regarded as interacting via mutual Yukawa repulsion and being confined by the potential due to neutralizing background [6–8] (see Appendix). When the system is uniform but within a cylinder, the latter potential has the cylindrical symmetry and, if the system is at sufficiently low temperatures, dust particles are organized into shell structures. Examples are shown in **Figs. 5** and **6**. These structures are expressed by simple interpolation formulas to a good accuracy [9].

In the case of dust particles in cylindrical discharge like PK-4J, we have an external field coming from the nonzero average charge density. When the density of dust particles is negligibly

small, we have the ambipolar field (14) as external potential for dust particles. With the increase of the density, the neutralizing background (average charge density of dust particles with the reversed sign) also becomes the source of the external potential. Since it is rather difficult to accurately estimate the external electrostatic potential or the contribution from the neutralizing background, we may evaluate two extreme cases where the external potential is given by that of ambipolar diffusion and the external potential completely flat (ideal uniform system).

As is shown in the previous Section, the charge neutrality becomes to be satisfied to a much better accuracy by the existence of dust particles. We therefore expect the ambipolar potential becomes weak and, among two limiting cases of external potentials, the flat external potential might be closer to the reality at least in the domain where we have dust particles. Since we already obtained the structures in the flat case by previous simulations, we adopt the ambipolar potential in our simulations and try to predict experimental results combining simulations in both cases.

5.2   Distribution in Ambipolar Potential and Effect of Gravity

In **Fig. 7**, we show some structures of dust particles in the ambipolar potential. We first note that the almost equal spacing between shells is also realized in this potential. In addition, as shown in the previous section, the charge neutrality becomes to be satisfied to a much better accuracy by the existence of dust particles, the ambipolar potential becomes weak. Therefore, we may apply the previous results for the structures in uniform cylindrical case.

When we have the gravitational force, these structures are influenced. The case of gravitation perpendicular to the symmetry axis may be convenient to observe the effect of gravity on the structures. With the increase of the gravity, the structure moves downward as a whole and the shells become compressed in the direction of the gravity as naturally expected.

Experiments on the ground, deformed shell structure has been
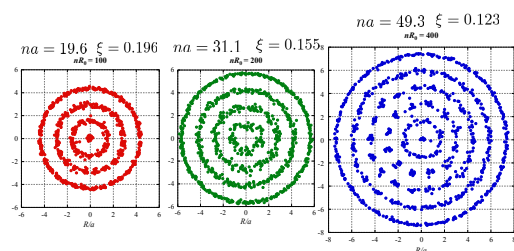
Fig. 5   Examples of shell structures in uniform cylinder (projection onto cross section)
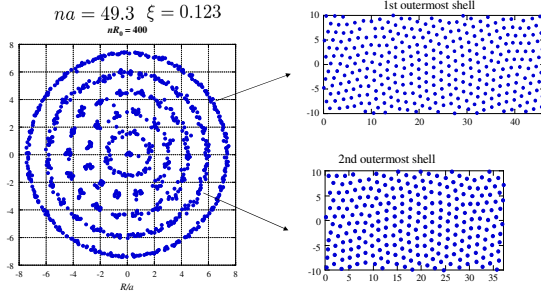
Fig. 6 Example of configuration within shells (cylinders cut-out into planes)
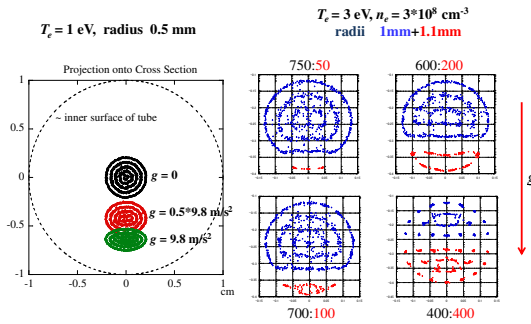
Fig. 7 Deformation and shift of center (left) and separation of particles with different radii

Fig. 8 Example of effect of anisotropic interaction. Cross sectional projection without anisotropic interaction (left), the one with anisotropic interaction (center), and cylinders (shells) cut-out into planes (right)

observed [10]. In our experiments [11], distributions of particles with circular cross section are observed under microgravity and deformed shells are observed on the ground. Our results seem not to be inconsistent with our theoretical works. For exact comparisons, however, some further improvement might be necessary.

When we have mixtures of dust particles of different radii, they are separated by gravitation, even if the difference is rather small as also shown in **Fig. 7**. In experiments, the system sometimes becomes a mixture of dust particles which are introduced and those non-intentionally exist.

5.3 Effect of Anisotropic Interaction

The electric voltage is applied to electrodes at both ends of the discharge tube and we have the flow of plasma along the axis with alternating direction. It is known that in this kind of alternating axial ion flow, the interaction between dust particles has an anisotropic part approximately expressed by [2]

$$-cM_t^2 \frac{(Q_\alpha e)^2}{r_{ij}^3} \exp(-r_{ij}/\lambda)(3\cos^2\theta_{ij}-1), \qquad (26)$$

where θ_{ij} is the angle between $\mathbf{r}_{ij}$ and the axis. The typical value of the ion thermal Mach number M_t is estimated to be around 0.5 from the discharge current of the order of 1 mA.

Structures of dust particles reflect the anisotropic part in their mutual interaction. An example is shown in **Fig. 8** where shells are developed into planes for observation of configuration on

shells. We observe that the triangular lattice with defects in the case of Yukawa interaction becomes oriented along the axis. When looked at along the direction of the axis, shells are decomposed into points, or uniformly distributed points on the circle are changed into lumps of dots on almost the same circle. The projected shell structure seems to change from concentric shells into a kind of lattice of lumps.

6. Conclusion

The behavior of dust particles in cylindrical discharges like PK-4J has been described based on both the drift-diffusion equations and numerical simulations. The former approach gives the behavior of densities of dust particles and the ambient plasma. We have enhanced charge neutrality where dust particles exist in comparison with the well-known case of ambipolar diffusion without dust particles. The condition for the void formation is expressed in terms of the particle radius, the electron temperature, and the electron density. Since we aim at the bulk system of dust particles without central void in our experiments by PK-4J, the results will be helpful to design experimental conditions.

The effect of discreteness of dust particles is analyzed by simulations. The structure formations are shown to be similar to those in the uniform cylindrical system previously investigated, giving almost equally spaced shells. The effect of the anisotropic part of mutual interaction between dust particles gives the alignment of the lattice structure on shells and eventually the alignment of particles along the axis. As a typical effect of gravity, the deformation and separation of particles of different radii have been shown as naturally expected. Details of the results can be used to identify physical parameters of the system.

References

1) V. E. Fortov, A. V. Ivlev, S. A. Khrapak, A. G. Khrapak, and G. E. Morfill, Physics Reports, **421** (2005) 1.

2) G. E. Morfill and A. V. Ivlev, Rev. Mod. Phys. **81** (2009)1353.

3) H. M. Thomas, G. E. Morfill, V. E. Fortov, A. V. Ivlev, V. I. Molotkov, A. M. Lipaev, T. Hagl, H. Rothermel, S. A. Khrapak, R. K. Suetterlin, M. Rubin-Zuzic, O. F. Petrov, V. I. Tokarev, and S. K. Krikalev, New J. Phys. **10** (2008) 033036.

4) For example, V. Fortov, G. Morfill, O. Petrov, M. Thoma, A. Usachev, H. Hoefner, A. Zobin, M. Kretschmer, S. Ratynskaia, M. Fink, K. Tarantik, Yu. Gerasimov, and V. Esenkov, Plasma Phys. Control. Fusion **47** (2005) B537.

5) G. E. Morfill, H. M. Thomas, U. Konopka, H. Rothermel, M. Zuzic, A. Ivlev, an J. Goree, Phys. Rev. Lett. **83** (1999)1598.

6) S. Hamaguchi and R. T. Farouki, J. Chem. Phys. **101** (1994) 9876.

7) Y. Rosenfeld, Phys. Rev. E**49** (1994) 4425.

8) H. Totsuji, C. Totsuji, T. Ogawa, and K. Tsuruta, Phys. Rev. E **71** (2005) 045401(R). H. Totsuji, T. Ogawa, C. Totsuji, and K. Tsuruta, Phys. Rev. E **72** (2005) 036406. T. Ogawa, H. Totsuji, C. Totsuji, and K. Tsuruta, J. Phys. Soc. Japan **75** (2006) 123501.

9) H. Totsuji and C. Totsuji, Phys. Rev. E **84** (2011) 015401(R).

10) S. Mitic, B. A. Klumov, U. Konopka, M. H. Thoma, and G. E. Morfill, Phys. Rev. Lett. **101** (2008)125002.

11) K. Takahashi, M. Tonouchi, S. Adachi and H. Totsuji: Int. J. Microgravity Sci. Appl., **31** (2014) 62.

Appendix: Potential in Uniform System

In the uniform system, the average densities of electrons, ions, and fine particles, $n_{e,i,\alpha}$, satisfy the the condition of the charge neutrality

$$n_i = n_e + Q_\alpha n_\alpha. \tag{27}$$

In this case, within the linear response, fine particles mutually interact via the Yukawa (Debye-Huckel) potential and are confined by the potential ϕ due to neutralizing background charge of the plasma $(n_i - n_e = Q_\alpha n_\alpha)$[6,7]. The potential energy is written[8] as the sum of

$$\sum_{i>j} \frac{(Q_\alpha e)^2}{4\pi\varepsilon_0 r_{ij}} \exp(-r_{ij}/\lambda) \tag{28}$$

and

$$(-Q_\alpha e)\phi(\boldsymbol{r}) = \int d\boldsymbol{r}' \frac{-(Q_\alpha e)^2 n_\alpha}{4\pi\varepsilon_0|\boldsymbol{r}-\boldsymbol{r}'|} \exp(-|\boldsymbol{r}-\boldsymbol{r}'|/\lambda). \tag{29}$$

We emphasize that the existence of the potential ϕ is sometimes overlooked in simple discussions of dusty plasmas. (Without ϕ, mutual repulsion of dust particles would lead to the explosion of the system: Since the whole system is charge neutral, this is certainly not the case.)

Particles develop their structure mutually repeling via the Yukawa potential and being confined by the potential $-(Qe)\phi$ of opposite charge background. For this kind of system with finite extention and cylindrical symmetry, the structures have been analyzed and expressed by simple interpolation formulas[9].